
JOURNAL OF THE AMERICAN CHEMICAL SOCIETY

Structural and Dynamic Characterization of Pro *Cis/Trans* Isomerization in a Small Cyclic Peptide

C. Francart, J.-M. Wieruszeski, A. Tartar, and G. Lippens*

Contribution from CNRS URA 1309, Pasteur Institute of Lille, 1 rue du Professeur Calmette, 59000 Lille, France

Received January 24, 1996[⊗]

Abstract: We describe the structure of a small cyclic peptide Cys-Leu-Pro-Arg-Glu-Pro-Gly-Leu-Cys containing two non-vicinal prolines. A previous HPLC analysis showed two well-resolved peaks at low temperature, and the hypothesis of slow conformational equilibrium due to steric constraints induced by cyclization was presented (Gesquiere, J.-C.; Diesis, E.; Cung, M. T.; Tartar, A. *J. Chromatogr.* **1989**, 478, 121). Our NMR study shows that at least three conformations of the peptide are present in solution: a major form which is the all-*trans* conformer and two minor forms where the peptide bonds Leu-Pro or Glu-Pro are in the *cis* conformation. The first HPLC peak was shown to contain the *trans-trans* and *trans-cis* forms of the peptide whereas the second HPLC peak contains the *cis-trans* form. The combined use of HPLC and NMR techniques led to the kinetic parameters characterizing the isomerization. The solution structure of the *trans-trans* peptide was determined by NMR spectroscopy and showed a predominant structural role for the proline in position three and for the cysteine bridge. Reduction of the disulfide bridge leads to a peptide where the *cis* and *trans* forms of both proline residues are still observable by NMR but where *cis/trans* isomerization of Pro3 is too fast to be detected on the HPLC time scale.

Introduction

The proline residue plays a unique role in peptide and protein structure through the conformational restriction introduced by its cyclic side chain and the small difference in free energy between the *cis* and *trans* conformers of the peptidyl-prolyl bond, allowing both conformations to be significantly populated.¹ The relevance of the simultaneous presence of both isomers will depend on the time scale of inversion of the Xaa-Pro bond, and this both for its biological role and physico-chemical detection.

In the context of cellular biology, the presence of significant amounts of *cis* isomers in the nascent peptide chains^{2,3} would

introduce a rate limiting step in the protein-folding process^{3,4} to such an extent that degradation of unfolded peptide may become inevitable. Therefore, *cis/trans* isomerization of Xaa-Pro bonds is generally catalyzed during protein folding by several enzymes known as peptidyl-prolyl *cis-trans* isomerases⁵ (PPIases) among which the best known are cyclophilin and FKBP.

The difference of chemical shift values corresponding to individual protons in both conformers is often larger than the

(4) (a) Brandts, J. F.; Halvorson, H. R.; Brennan, M. *Biochemistry* **1975**, 14, 4953. (b) Brandts, J. F.; Lin, L. N. *Methods Enzymol.* **1986**, 131, 7. (c) Briggs, M. S.; Roder, H. *Proc. Natl. Acad. Sci. U.S.A.* **1992**, 89, 2017.

(5) (a) Schmid, F. X.; Baldwin, R. L. *Proc. Natl. Acad. Sci. U.S.A.* **1978**, 75, 4764. (b) Handschumacher, R. E.; Harding, M. W.; Rice, J.; Drugge, R. J. *Science* **1984**, 226, 544. (c) Fischer, G.; Wittmann-Liebold, B.; Lang, K.; Kiefhaber, T.; Schmid, F. X. *Nature* **1989**, 337, 476. (d) Siekierka, J. J.; Hung, S. H. Y.; Poe, M.; Lin, C. S.; Sigal, N. H. *Nature* **1989**, 341, 755. (e) Harding, M. W.; Galat, A.; Ueling, D. E.; Schreiber, S. L. *Nature* **1989**, 341, 758. (f) Galat, A. *Eur. J. Biochem.* **1993**, 216, 689.

* To whom correspondence should be addressed.

⊗ Abstract published in *Advance ACS Abstracts*, July 1, 1996.

(1) Wüthrich, K.; Grathwohl, C. *FEBS Lett.* **1974**, 43, 337.

(2) Evans, P. A.; Kautz, R. A.; Fox, R. O.; Dobson, C. M. *Biochemistry* **1989**, 28, 362.

(3) Schreiber, G.; Fersht, A. R. *Biochemistry* **1993**, 32, 11195.

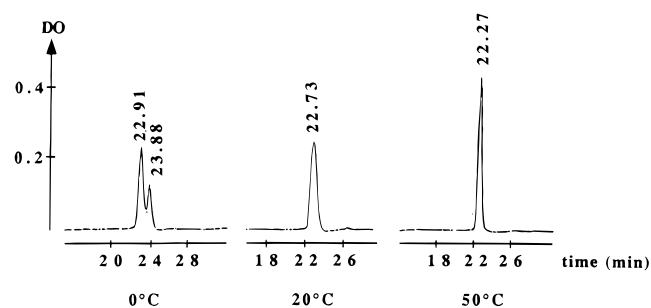
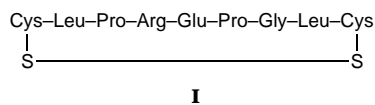


Figure 1. HPLC profiles of peptide **I** at 0, 20, and 50 °C.

inversion rate, leading to a simultaneous observation of both forms by NMR spectroscopy. Increasing the inversion rate by increasing the temperature may, in some cases, induce coalescence of the corresponding signals. Although much less frequently observed, the time scale of the *cis*–*trans* inversion may increase to such an extent that it becomes observable on the time scale of the HPLC technique, with significant distortions of the elution profiles.⁶ This phenomenon is important for purity assessment of synthetic peptides and could become increasingly frequent with the development of faster separation methods.

Several peptides containing two vicinal proline residues⁷ or sterical constraints induced by a disulfide bridge⁸ endow such a slow conformational equilibrium detectable by HPLC. The HPLC profile of the 9 amino acids long disulfide-bridged peptide⁸ (**I**) under study here,



typically illustrates the effect of the inversion rate on the aspects of the HPLC peaks. Peptide **I** elutes as a broad peak at 20 °C (Figure 1). Decreasing the temperature to 0 °C leads to two separated peaks although some coalescence can still be observed. On the contrary, increasing the temperature to 50 °C leads to a single sharp peak. The linear peptide, in which the disulfide bridge has been reduced, elutes even at low temperature as a single sharp peak, indicating an important role for the cyclic constraint on the HPLC behavior.

In this report, we first examine by HPLC the influence of the solvent on the equilibrium population of peptide **I**. We extend this description by a detailed NMR study of the different conformers in equilibrium, demonstrate that both prolines are present in the *trans* and *cis* forms, and determine the structure of the all-*trans* conformer. Both techniques of HPLC and NMR are combined to estimate the isomerization rate (k_{iso}) of the different conformers. Finally, the influence of the structural constraint imposed by the disulfide bridge is examined through the NMR analysis of the reduced peptide: although three conformers could still be detected by NMR in the reduced peptide, opening the disulfide leads to an increased interconversion rate, in agreement with the original hypothesis⁸ of the importance of structural constraints imposed by cyclization.

(6) (a) Melander, W. R.; Jacobson, J.; Horvath, C. *J. Chromatogr.* **1982**, *234*, 269. (b) Jacobson, J.; Melander, W. R.; Vaisnys, G.; Horvath, C. *J. Phys. Chem.* **1984**, *88*, 4536. (c) Nishikawa, T.; Hasumi, H.; Suzuki, S.; Kubo, H.; Ohtani, H. *Chromatographia* **1994**, *38*, 359.

(7) Rusconi, L.; Perseo, G.; Franzoi, L.; Montecucchi, P. C. *J. Chromatogr.* **1985**, *349*, 117.

(8) (a) Gray, W. R.; Rivier, J. E.; Gaylean, R.; Cruz, L. J.; Olivera, B. M. *J. Biol. Chem.* **1983**, *258*, 12247. (b) Gesquiere, J.-C.; Diesis, E.; Cung, M. T.; Tartar, A. *J. Chromatogr.* **1989**, *478*, 121.

Experimental Procedures

Peptide Synthesis. The peptide was synthesized with an Applied Biosystem 430 A synthesizer using classical solid-phase methodology⁹ on a BocCys(4-CH₃Bzl)OCH₂Pam resin (0.73 mM/g). The protected peptide resin (0.25 mM) was synthesized by double coupling, with deprotection by trifluoroacetic acid (TFA) and neutralization with diisopropylethylamine (DIEA) of N^α-Boc-Cys(4-MeBzl)-resin, N^α-Boc-Leu, N^α-Boc-Gly, N^α-Boc-Pro, N^α-Boc-Glu(cHex), N^α-Boc-Arg(Tos), N^α-Boc-Pro, N^α-Boc-Leu, and N^α-Boc-Cys(4-MeBzl). Hydroxybenzotriazole active ester was used for coupling reactions and the double coupling step was followed by capping with acetic anhydride. After coupling of the last amino acid, the N^α-Boc protecting group was removed, the amino acid neutralized with DIEA, and the peptide resin dried *in vacuo*. This peptide resin was cleaved with 10 mL of liquid HF and 0.75 g of *p*-cresol and 0.25 g of *p*-thioanisol at 0 °C under agitation for 1 h 30 min. The product was washed with ethyl ether, extracted with 5% aqueous acetic acid, and lyophilized.

Peptide Purification. HPLC purification of the cyclic peptide being difficult due to peak broadening, purification was first performed on the reduced peptide by high performance liquid chromatography (HPLC) at room temperature on a reversed-phase C₁₈ column (10 × 500 mm) at a flow rate of 2 mL/min using a water/acetonitrile gradient from 0% to 36% CH₃CN in 0.05% aqueous TFA in 80 min. The apparatus consisted of two Shimadzu LC-6A pumps (solvent A: 0.05% of TFA, solvent B: 60% of CH₃CN + 0.05% of TFA), a Shimadzu SCL-6A system manager, and a Shimadzu SPD-6A UV detector (λ = 215 nm).

Purity was assessed by analytical HPLC at room temperature on a C₁₈ column (Vydac 218TP, 3 × 250 mm) at a flow rate of 0.7 mL/min using a water/acetonitrile gradient from 0% to 60% CH₃CN in 30 min in 0.05% aqueous TFA. Mass spectra of the purified peptide acquired on a Plasma Desorption Mass Spectrometer (PDMS) Bio-Ion 20 revealed a mass value (M + H)_{obs} 988, in agreement with the theoretical prediction (M + H)_{calc} 988.

Cyclization. The purified linear peptide was cyclized by dissolving 140 mg of lyophilized powder in 1.5 L of a 10⁻² M ammonium bicarbonate solution (pH adjusted with aqueous ammonia to 9) followed by air bubbling for 4 days at room temperature. Samples of the reaction environment were analyzed by analytical HPLC during the oxidation in order to follow the peptide cyclization. The peptide concentration was kept low (10⁻⁴ M) in order to favor the first-order reaction (intramolecular disulfide bridge formation) versus the second-order reaction (dimerization).

The cyclized peptide was purified in similar conditions as the linear peptide. Differences were the temperature (0 °C), the solvent A containing 5% of CH₃CN and 0.05% of TFA in order to avoid solvent freeze in the column, and the water/acetonitrile gradient from 5% to 21.5% CH₃CN. Operating at 0 °C leads to a better separation of the peaks and the elimination of impurities which were eluted at a retention time contained between those of the two isomers. The purified cyclic peptide was then lyophilized, analyzed by analytical HPLC and mass spectroscopy (M + H)_{obs} 986, and stored at -15 °C.

HPLC Experiments. Peptide solutions were prepared in advance in order to allow the *cis/trans* isomerization to reach an equilibrium before injection. HPLC profiles of the peptide were obtained at three different column temperatures (0, 20, and 50 °C), on a similar apparatus as used for the peptide purification. A C₁₈ column (Vydac 218TP, 3 × 250 mm) was first immersed in a constant temperature bath at 0 °C, then left at room temperature or warmed at 50 °C. Twenty microliters of an aqueous solution containing 1 mg/mL of peptide were injected. The peptide was eluted at a flow rate of 0.7 mL/min with a water/acetonitrile gradient from 0% to 100% of solvent B in 30 min (solvent A: 5% of CH₃CN + 0.05% of TFA, solvent B: 60% of CH₃CN + 0.05% of TFA) and the column effluent was monitored at 215 nm.

For the study at 0 °C of the peptide in an aqueous solution containing 50 mM sulfate or phosphate at different pH or in a mixed solution H₂O/CD₃CN (21.5%), 20 μL of a 3 mM solution of peptide were injected with the same parameters as in the previous experiments but under isocratic conditions (30% of solvent B).

(9) Merrifield, R. B. *J. Am. Chem. Soc.* **1963**, *85*, 2149.

A previous study¹⁰ had shown that a solution of lithium chloride in THF increased the population of the *cis* isomer from 12% to approximately 35–40%. We performed a similar experiment by HPLC analysis at 0 °C of the peptide dissolved in a 300–400 mM LiCl/THF solution. In order to avoid all moisture traces, the peptide was dried *in vacuo* over P₂O₅ at room temperature. THF (Janssen Chimica) was distilled over sodium before use; LiCl (Merck) was dried *in vacuo* at 300 °C. Solutions were prepared under an argon atmosphere.

NMR Sample Preparation. NMR samples were prepared by dissolving the peptide in a 50 mM sulfate aqueous solution or in a 21.5% (v/v) CD₃CN/H₂O solution. Final peptide concentrations were 2 or 8 mM. The pH of the samples was adjusted with concentrated NaOD and DCl to 3.5 for the aqueous solution and to 2 for the CD₃CN/H₂O solution. The latter value is that of the eluent solution at the HPLC column exit. Chemical shifts were referenced with respect to TMSP (trimethylsilyl propionate).

NMR Spectra Acquisition. All NMR spectra were acquired on a Bruker DMX600 spectrometer at 277 K. Data were processed using the SNARF software (F. H. J. van Hoesel, University of Groningen, The Netherlands) or the Bruker UXNMR software on a R4000 Silicon Graphics workstation.

Homonuclear ¹H TOCSY and NOESY spectra were acquired using 2048 × 512 complex points in the ω₂ and ω₁ dimensions respectively for a total spectral width of 12 ppm, whereas 8192 complex points in the ω₂ dimension were collected for the DQFCOSY spectrum. Mixing times were 80 ms MLEV spin-lock time for the TOCSY spectrum and 100, 200, 300, 400, and 600 ms delays for the NOESY spectra.

Water suppression in the homonuclear spectra was performed using gradient techniques in the NOESY water flip-back WATERGATE sequence.¹¹

The kinetics studies were performed in an aqueous solution of protonated acetonitrile. We used a WATERGATE sequence with two selective inversion pulses on both intense proton resonances combined with a double low-power pre-irradiation in order to eliminate the solvent resonances.

Heteronuclear spectra (HSQC, HSQC-TOCSY) were collected with 2048 × 1024 complex points for 12 ppm in the ¹H dimension and 100 ppm in the ¹³C dimension.

Determination of Distances. Interproton distances were determined on the basis of the NOESY data acquired for four different mixing times: 100, 200, 300, and 400 ms. Peak volumes were converted into distances using a routine incorporated in the program SNARF as previously described.¹²

The recent method of off-resonance ROESY¹³ was used to confirm the previously obtained distance values. This technique allows the measurement of the dipolar cross-relaxation rates along an effective field axis in the rotating frame tilted by an angle θ with respect to the static magnetic field. By varying this angle from zero (NOESY case) to higher values (more ROESY contributions), the longitudinal (σ) and transverse (μ) dipolar cross-relaxation rates can be determined with a high accuracy since they result from a fitting procedure. The spectra were recorded as a series of 2D spectra with a constant spin-lock field strength γB₁ = 7 kHz but with varying offset Δ of the spin-lock field. Eleven values of θ = arctg(γB₁/Δ) were sampled between 5° and 55°, with three mixing times of 50, 100, and 200 ms for every angle. Buildup curves were determined independently for every angle, using the cross-peak volumes normalized to the diagonal peak volumes in order to extend the validity of the initial slope approximation.¹⁴ A least-squares fit of the resulting slopes as a function of the angle θ to the theoretical expression σ' = σ cos²(θ) + μ sin²(θ) yields both relaxation rates.

(10) Kofron, J. L.; Kuzmic, P.; Kishore, V.; Colon-Bonilla, E.; Rich, D. H. *Biochemistry* **1991**, *30*, 6127.

(11) (a) Piotto, M.; Saudek, V.; Sklenar, V. *J. Biomol. NMR* **1992**, *2*, 661. (b) Lippens, G.; Dhalluin, C.; Wieruszkeski, J. M. *J. Biomol. NMR* **1995**, *5*, 327.

(12) Lippens, G.; Najib, J.; Wodak, S. J.; Tartar, A. *Biochemistry* **1995**, *34*, 13.

(13) (a) Desvaux, H.; Berthault, P.; Birlirakis, N.; Goldman, M.; Piotto, M. *J. Magn. Reson., Ser. A* **1995**, *113*, 47. (b) Desvaux, H.; Berthault, P.; Birlirakis, N. *Chem. Phys. Lett.* **1995**, *233*, 545.

(14) Macura, S.; Farmer, B. T., II; Brown, L. R. *J. Magn. Reson.* **1986**, *70*, 493.

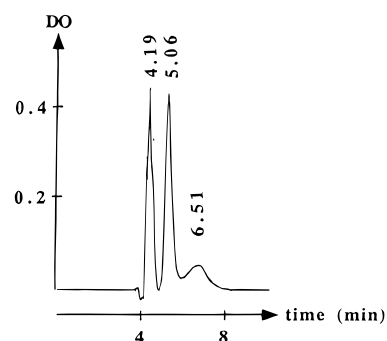


Figure 2. HPLC profile at 0 °C of the peptide dissolved in a LiCl/THF solution. Subtraction of the solvent profile and peak integration were performed with a Shimadzu C-R 3A integrator.

Generation of Structures. All structures were generated with the X-PLOR program.¹⁵ We first used the subembedded algorithm, where the subembedded set was extended to the δ carbons because of the presence of NOE's contacts involving the methyl group of Leu8. The covalent constraints concerning the disulfide bridge were eliminated at this stage and were reintroduced as fake NOE distances. NOE constraint terms were calculated using a split harmonic energy term with a force constant of 50 kcal/(mol·Å²). After the subembedding, a simulated annealing step was performed on every structure, consisting of a thousand steps at 2000 K followed by a cooling down during another 1000 steps to room temperature. Finally these structures were refined by a simulated annealing protocol with a starting temperature of 1000 K and a total number of 1000 steps during cooling. Among all these structures, only those with no NOE violations larger than 0.5 Å were kept and used for the structural comparisons.

Visual superimposition and comparison of all structures were performed with the INSIGHTII module of the BIOSYM package running on a R4000 Silicon Graphics workstation.

Results and Discussion

HPLC Experiments. Subambient temperatures are required in order to observe two separated peaks in the HPLC pattern of peptide **I**. The ratio of peaks in the resulting chromatogram represents the ratio of isomers in the injection solvent, provided isomers have different retention time and temperature is low enough to slow down isomerization during the elution.

Therefore, low-temperature HPLC was used to investigate the influence of pH and salts on the equilibrium in aqueous solution. Neither pH variation (from 2 to 8) nor the choice of salt (phosphate or sulfate solution) had a significant influence on the chromatogram. When the aqueous solution was replaced by a mixed H₂O/CD₃CN solution, a very similar chromatogram with two peaks in the previously obtained ratio 75:25 was obtained. Only when peptide **I** was initially dissolved in a 300–400 mM anhydrous LiCl/THF solution was a significant modification of the HPLC profile observed (Figure 2). All three peaks contained peptide **I** according to the PDMS analysis. The ratio of the peaks (33:46:21) seems consistent with a general increase in the percentage of the *cis* isomers of both proline residues, confirming the role of LiCl/THF as a promoter of the *cis* isomer population.¹⁰

NMR Assignments of the Different Conformational Isomers in CD₃CN. An initial structural study of the peptide was performed in similar conditions as exist at the HPLC column exit, a 21.5% (v/v) acetonitrile solution at pH 2. In order to facilitate the NMR study, we used deuterated acetonitrile in H₂O or D₂O.

(15) Brünger, A. T. *X-PLOR Version 3.1 Manual*; Yale University: New Haven, CT, 1992.

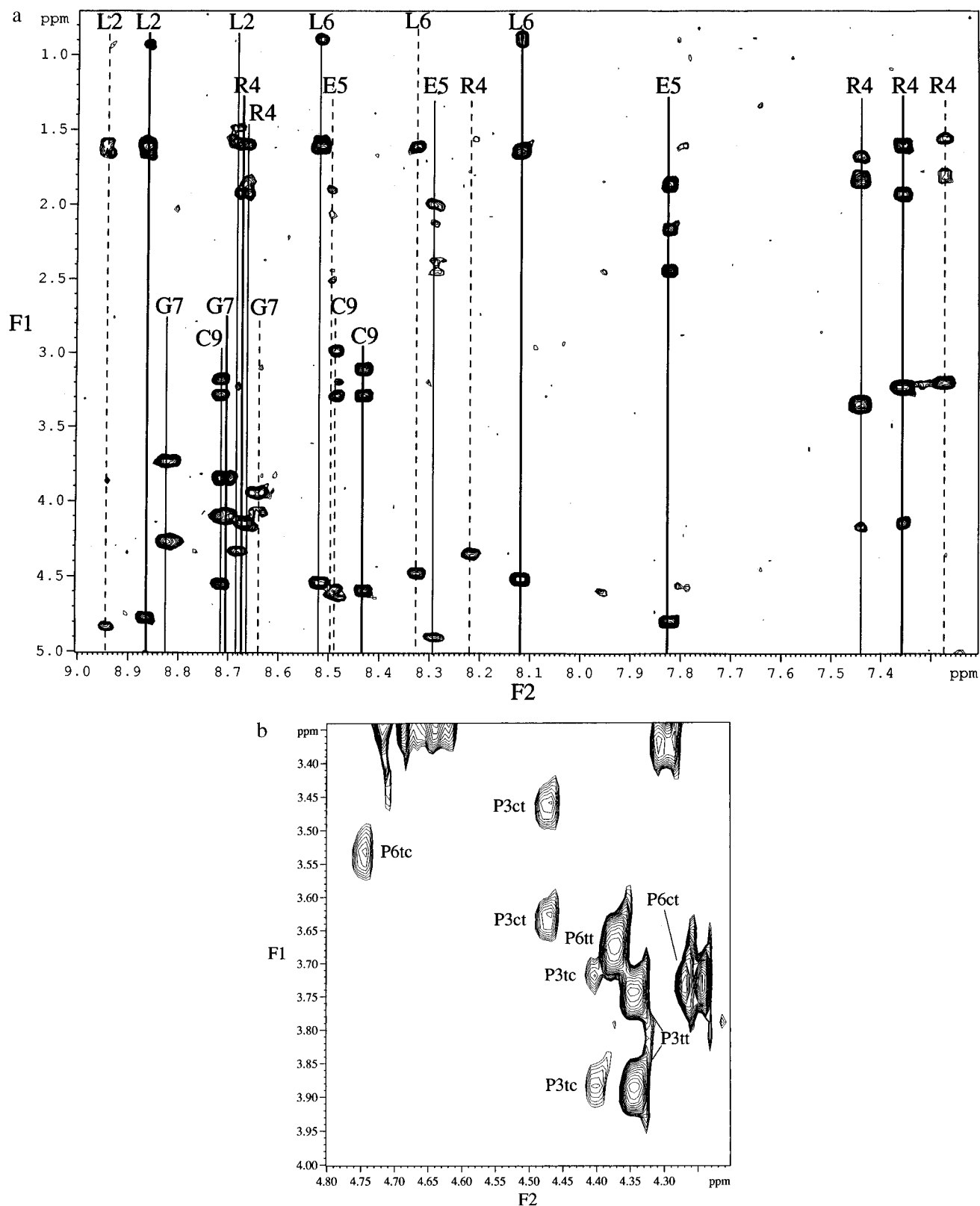


Figure 3. (a) Amide region showing the NH resonances in a 80-ms TOCSY spectrum in H₂O at 277 K. As the results in aqueous solution and in a water/acetonitrile solution varied very little, we show here the spectrum in H₂O, which presents the best separation of resonance lines. Bold lines correspond to the resonance lines of the *trans-trans* form, full thin lines to those of the *cis-trans* form, and dotted lines to those of the *trans-cis* form. (b) Aliphatic region showing the α proton resonances of the proline residues in a 80-ms TOCSY spectrum in CD₃CN/D₂O at 277 K for the three forms: *trans-trans* (tt), *cis-trans* (ct), and *trans-cis* (tc).

Whereas the HPLC pattern suggested the presence of two isomers, the analysis of the NMR spectra in CD₃CN reveals the existence of at least three isomers. The three conformers could be readily identified on the basis of the several distinct sets of proton resonances in the TOCSY spectra: starting from

the amide proton resonances, we observed 6 TOCSY lines corresponding to the 2 leucines and 3 sets of H resonances for the glutamic acid, the glycine, the arginine, and the C-terminal cysteine (Figure 3a). The presence of six proline spin systems in the aliphatic part of the TOCSY spectra (Figure 3b) confirmed

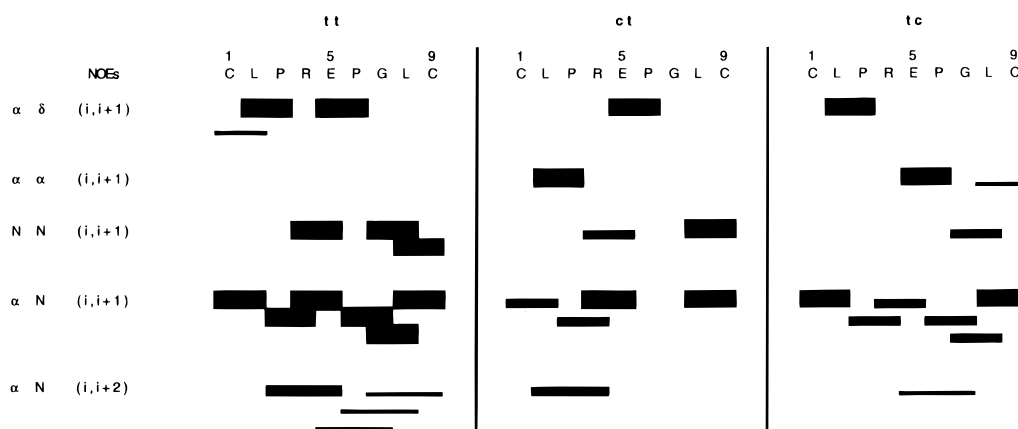


Figure 4. Summary of sequential and nonsequential NOE's for the three different conformers of the peptide: *trans-trans* (tt), *cis-trans* (ct), *trans-cis* (tc).

the presence of three isomers, and agreed well with the original hypothesis of a slow Pro isomerization as the origin of the structural diversity.

The assignment of the six proline spin systems to the three isomers was based on their characteristic contacts to the preceding residue (α - δ for *trans*-Pro, α - α for *cis*-Pro).¹⁶ The proline in position 3 follows a leucine and was found twice in the *trans* and once in the *cis* conformation, and the proline in position 6, following a glutamic acid, was equally found twice in the *trans* and once in the *cis* conformation.

Connecting the proline residues through the network of sequential and nonsequential NOE's, we were able to identify a major form where the two prolines are in the *trans* conformation (tt form, Figure 3) and two minor forms where the prolines are respectively *cis-trans* (ct form, Figure 3) and *trans-cis* (tc form, Figure 3). Complete assignments for all residues were established.

An alternative probe for the conformation of the proline residue is given by the ¹³C chemical shift values of the proline β and γ carbons and by the α carbon chemical shift of the preceding residue. Indeed, the $C\beta$ and $C\gamma$ chemical shifts of a *cis*-proline are about 1 ppm downfield and 2 ppm upfield, respectively, of the corresponding shifts for the *trans*-proline.¹⁷ A downfield shift for the $C\beta$ carbons of the *cis*-proline residues higher than 1 ppm was observed (data not shown). The chemical shift values for the $C\gamma$ carbons could not be measured since the corresponding cross-peaks showed heavy overlap. The $C\alpha$ chemical shift of the residue preceding a *trans*-proline is about 2 ppm upfield from its characteristic value.¹⁸ We noted a $C\alpha$ chemical shift of the leucine in position 2 preceding a *trans*-proline equal to 52.5 ppm versus the value of 53.8 ppm in a random peptide,¹⁹ whereas no difference to the random chemical shift was observed for the leucine in position 2 preceding a *cis*-proline.

Structure Calculation. The final set of NOE restraints for the major *trans-trans* isomer (tt) consisted of 45 intraresidue constraints and 52 interresidue constraints. Of the latter, 37 were sequential constraints and 15 nonsequential constraints, with 7 contacts between protons that are three residues apart and 3 that are five or more residues apart. The most important of these contacts are summarized in Figure 4.

For the two minor forms (ct and tc), only 60 distance constraints, divided into 40 intraresidue and 20 interresidue pairs, were observable for the *cis-trans* form and 42 distances constraints with 25 intraresidue and 17 interresidue constraints for the *trans-cis* isomer (Figure 4). This lower number of NOE contacts observed is not necessarily due to a lesser degree of structuring but can be ascribed to the low concentrations of both minor forms (*vide infra*). As for the weak constraints between protons that are three residues or more apart, we could identify unambiguously no more than two contacts in both forms: for the ct form one characterizing the disulfide bridge (Cys9(H α)-Cys1(H β)) and one important NOE contact between the α protons of Glu5 and Cys9, and for the tc form two NOE contacts between Pro6(H α)-Cys9(H α) and Arg4(H α)-Leu8(H δ).

The distances of the tt form were classified into three classes, corresponding to distance ranges of 2–2.8 Å (strong), 2–3.5 Å (medium), and 2–5 Å (weak). However, as the number of NOE contacts is necessarily more limited in a small peptide than in a globular protein, a more accurate determination of the distance constraints is needed.²⁰ A first step to obtain narrower distance constraints than those obtained by the three-step classification used the buildup rates of the various NOE contacts and the comparison with the proline δ - δ distance as a reference. As a next step, we performed a series of off-resonance ROESY spectra¹³ to validate these distances. This technique allows buildup rates in both the laboratory and rotating (spin-locked) frame to be obtained if volumes of cross and diagonal peaks can be determined. However, we faced a severe problem of overlap at the level of the diagonal peaks, and could therefore only determine a limited number of distances by this method. Still, the good agreement between both methods (Table 1) gave us some confidence in the narrower distance ranges obtained through the buildup curve calibration. A range of ± 0.3 Å around the measured distance was taken for those constraints that involve only backbone protons, whereas it was loosened to ± 0.5 Å for those contacts involving side-chain protons in order to allow for the effect of increased mobility.

The values of the J coupling constants as measured on the DQFCOSY spectrum are shown in Table 2. However, in the calculation for the tt molecule, only the backbone ϕ dihedral angles for the residues Leu2 and Glu5 were restrained, as they correspond to high values of the J coupling constant. For all other residues, the measured ³J_{NH α values corresponded to a more averaged value, and the corresponding ϕ angles were therefore not constrained.}

(16) Wüthrich, K. *NMR of Proteins and Nucleic Acids*; John Wiley and Sons: New York, 1986.

(17) Howarth, O. W.; Lilley, D. J. M. *Prog. Nucl. Magn. Reson. Spectrosc.* **1978**, *12*, 1.

(18) Clore, G. M.; Bax, A.; Driscoll, P. C.; Wingfield, P. T.; Gronenborn, A. M. *Biochemistry* **1990**, *29*, 8172.

(19) Richarz, R.; Wüthrich, K. *Biopolymers* **1978**, *17*, 2519.

(20) Kazmierski, W. M.; Yamamura, H. I.; Hruby, V. J. *J. Am. Chem. Soc.* **1991**, *113*, 2275.

Table 1. Interproton Distances (Å) Measured with the Routine in the SNARF Program and with the Off-Resonance ROESY Method

distance (Å)	buildup	off-ROESY
NH Arg4–NH Glu5	2.35	2.57
NH Glu5–Ha Glu5	3.24	2.90
NH Gly7–Ha Pro6	1.92	2.15
NH Gly7–NH Leu8	2.42	2.71
NH Leu8–Ha Gly7	2.38	2.48
NH Leu8–Ha Gly7	2.51	2.66
NH Leu8–Ha Leu8	2.73	2.72
NH Cys9–NH Leu8	2.51	2.65
NH Cys9–Ha Leu8	2.06	2.17
NH Cys9–Ha Cys9	2.27	2.59
NH Cys9–Hb Cys9	2.53	2.54

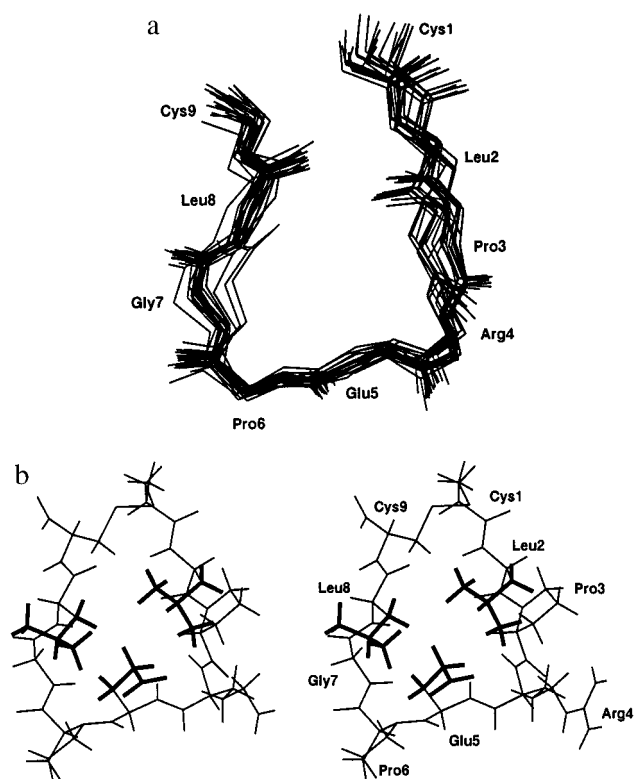
Table 2. $^3J_{\text{NH}\alpha}$ Coupling Constants (Hz) for the Three Different Conformers of the Peptide: *Trans–Trans* (tt), *Cis–Trans* (ct) and *Trans–Cis* (tc)

<i>J</i> (Hz)	tt obs	ct obs	tc obs
Leu2	9.2	6.5	9.2
Arg4	6.3	6.5	9.8
Glu5	9.6	9.1	/
Leu8	6.3	9.2	9.8
Cys9	7.7	7.7	7.9

Both NOE and dihedral angle constraints were introduced as structural constraints into the X-PLOR program.¹⁵ A total of 100 structures was generated. Of the 100 structures, 54 had no violations larger than 0.5 Å. By superimposing these accepted structures with INSIGHTII, two families of structures were observed. One family presented short interproton distances between Leu8(H α) and Pro3(H α). Although the corresponding cross peak could possibly be attenuated by an enhanced mobility, the fact that the contact involves only backbone atoms made this hypothesis not very probable. Direct experimental evidence, however, of the true absence of such a short distance came from the off-resonance ROESY spectra at high angle, where the cross-relaxation rate in the rotating frame is dominant.¹³ No cross peak could be observed between the aforementioned protons, allowing us to impose a lower bound of 4.5 Å for both distances. A new XPLOR run effectively eliminated one of the subfamilies, and left us with 22 structures that presented no violation larger than 0.5 Å.

The superimposed structures for the tt molecule are shown in Figure 5a. The root mean square (rms) deviation from the average structure was 0.46 Å for backbone heavy atoms and 1.10 Å for all non-H atoms. These results show that the backbone structure is well-defined, in agreement with the original hypothesis that cyclization considerably reduces the flexibility of the peptide. In agreement with the observed coupling constants, the spread in dihedral angles is small for Leu2, the first residue following the disulfide bridge, and for Glu5 and Pro6, the residues *i* and *i* + 1 of the central β -turn (*vide infra*), whereas it is larger for the other residues, reflecting the absence of dihedral angle constraints.

The *trans–trans* molecule is characterized by a β -turn centered around the proline in position 6 and the glycine in position 7. Indeed, the distance between the α carbons of Glu5 and Leu8 is shorter than 7 Å, and neither residue Pro6 nor Gly7 is in a α -helical region. We could not clearly distinguish the β -turn type: the difference between a type II and a type IV turn is based on the ψ angle of the *i* + 1 residue,²¹ but in our structures this angle oscillates around the border value of 60°. The *i* + 2 Gly7 residue is characterized by positive (ϕ, ψ) angles, which is a common conformation for this residue in a turn.²¹

**Figure 5.** (a) Superposition of backbones of the 22 structures generated for the peptide *trans–trans*. (b) Stereoview of the peptide showing the cluster formed by the side chains of the two leucines and the glutamic acid.

The turn conformation is further confirmed by a number of NOE contacts between the side chains of Leu8 and Glu5. Moreover, the side chain of Leu2 joins the two aliphatic side chains to form a hydrophobic cluster, as is confirmed by the weak contact between the Leu8 β and γ protons toward the δ methyl groups of Leu2. This leads to the picture where the two leucine residues and the glutamic acid present their side chains to one side of the backbone cycle, whereas the arginine residue is completely solvent exposed (Figure 5b).

For the two minor forms, the reduced number of constraints combined with a severe overlap of diagonal peaks impeding any accurate distance measurement makes a complete structure determination nearly impossible. However, from the combined data of NOE's, coupling constants, and chemical shift values we can qualitatively describe both minor forms.

The N-terminal Leu2 residue is in a similar conformation in the tt and tc molecule, as is proven by both the high value of its coupling constant and the strong $\alpha\text{N Cys1(H}\alpha\text{)}\text{--Leu2(NH)}$ NOE contact, as well as by the almost identical chemical shift values of all protons. However, for the ct molecule, a decrease of 3 Hz for its $^3J_{\text{NH}\alpha}$ coupling constant together with the weaker $\alpha\text{N(1,2)}$ contact points to a different conformation for Leu2. This is confirmed by the chemical shift values for the α proton of this residue: it is shifted upfield by 0.6 ppm for the ct form. Therefore, the conformation of the N-terminal residue seems solely determined by the Pro3 conformation, independent of the Pro6 state.

Considering the $^3J_{\text{NH}\alpha}$ values for Leu8, the conformation of the C-terminal Leu residue seems to have undergone a considerable change in both tc and ct forms compared to the tt molecule. The presence in the ct form of a strong NH–NH contact between Leu8 and Cys9, together with the presence of a long-range contact between Glu5(H α) and Cys9(H α), indicates that

(21) Wilmot, C. M.; Thornton, J. M. *J. Mol. Biol.* **1988**, *203*, 221.(22) Hodel, A.; Kautz, R. A.; Fox, R. O. *Protein Sci.* **1995**, *4*, 484.

the turn has shifted to the Pro6-Gly7-Leu8-Cys9 quadruplet in the *ct* form. The amazing fact here is that the conformation of the Pro3 has structural consequences beyond the Pro6, and thus induces a more global change of the peptide conformation.

For the *tc* form, the lack of any strong NH–NH contact (Figure 4) indicates the absence of a regular turn structure. However, the long-range contact between Arg4(H α) and Leu8(H δ) points to a more compact structure with N- and C-termini brought closer together through the *cis* form of Pro6.

Kinetics. The apparent contradiction between the two HPLC peaks and the three conformers detected by NMR can be explained in two different ways: the time scale for interconversion could be simultaneously slow for NMR but rapid for the HPLC technique, or alternatively, both Xaa–Pro bonds could be characterized by a very slow isomerization rate but only two isomers have retention times different enough to be separated by chromatography.

In order to quantify the kinetics of the interconversion, a direct analysis by NMR of the content of the two HPLC peaks was performed. In addition to the column, we cooled the peak collecting area in order to avoid reisomerization of the content of each peak. Samples (1 mg) of the cyclic peptide were injected on a HPLC column maintained at 0 °C. The two peaks were collected separately and directly analyzed by NMR at 4 °C. Series of 1D spectra were collected at different time periods.

In the 1D spectra corresponding to the large HPLC peak, the resonances of the *trans–trans* isomer could be easily identified, but the low gain imposed by the protonated solvent (an aqueous solution of protonated acetonitrile) made the identification of any minor form rather ambiguous. The increase of the arginine Arg4_{tt} signal of the *trans–trans* form and the decrease of the arginine Arg4_{ct} signal of the *cis–trans* form as a function of time during the NMR analysis of the second peak (Figure 6a), however, demonstrated the attribution of the *cis–trans* form to the second peak. The time scale of the interconversion process from the *ct* form to the *tt* form was deduced from the buildup of several *tt* resonances and the concomitant decrease of the *ct* resonances in the 1D spectra of Figure 6a. When modeling these curves by a monoexponential curve, we obtain a characteristic time constant of the order of 4 h for the *ct–tt* interconversion (Figure 6b).

The absence of the Leu2_{tc}, Arg4_{tc}, and Leu8_{tc} signals in the initial spectra of the sample corresponding to the second HPLC peak and their gradual appearance as a function of time clearly show that this second HPLC peak contains only the *ct* form, but does not give information about the kinetics of the *tt–tc* interconversion. High-temperature spectra recorded on an aqueous sample indicated a gradual coalescence of the Leu2_{tt} and Leu2_{tc} NH resonances when increasing the temperature from 308 to 343 K. A series of 2D TOCSY spectra at these higher temperatures (data not shown) confirmed this intermediate exchange at the NMR time scale for the *tt* and *tc* forms at 343 K, whereas no coalescence at all was observed for the *ct* form. This observation shows that even in H₂O the *cis/trans* isomerization of Pro3 remains very slow, and is consistent with a more rapid interconversion of *tt–tc*, which would lead to simultaneous elution of the *tc* and *tt* forms in the first HPLC peak. These kinetic data confirm the results from our structural analysis that indicated a global conformational change for the peptide upon *cis/trans* isomerization of Pro3.

NMR Results in H₂O. The peptide under study here contains two solvent-exposed proline residues with different activation barriers, that can even be lowered by removing the structural constraint imposed by the cyclization (*vide infra*). These factors make it an important substrate to study the catalytic effect of

the peptidyl–prolyl isomerases. The crystal structure of cyclophilin A complexed with different substrates shows the bound proline in the *cis* conformation.²³ However, it is not clear to what extent these flexible substrates can adequately mimic the *cis*-proline in an unfolded or partially folded polypeptide. It will be most interesting to see whether cyclophilin binds preferentially to one of the proline residues in the *cis* form, and whether it effectively can lower the *cis/trans* isomerization barrier. Therefore we repeated the NMR analysis of the free peptide in conditions nearer to those in which the enzyme acts: an aqueous solution with a pH value higher than 4. No noticeable differences for chemical shift values and NOE pattern were observed, in agreement with the earlier HPLC results. We thus believe that our previous conclusions about the presence and conformation of the three conformers in the water/acetonitrile solution can be readily extended to the peptide in aqueous solution.

Relative populations as obtained by integration of the HPLC elution peaks indicated no influence on the initial solvent (Table 3), but could only estimate the ratio of (*tt* + *tc*):*ct*. Integration of the glycine vicinal H α 1–H α 2 resonances in 2D NOE spectra allows an estimate of the individual populations of the three conformers, in the hypothesis of similar cross- and self-relaxation rates. The ratios obtained by HPLC and NMR methods in water are in good agreement, and confirm the presence of the *tt* and *tc* forms in the first HPLC peak. On the basis of the NMR estimates, acetonitrile seems to favor slightly the *tt* form, but this conclusion remains highly ambiguous due to uncertainties on the ratios given.

Hodel et al. proposed a simple “ β carbon rule” to explain the preference for the *cis*-form of the Lys116–Pro117 bond in the constrained loop of Staphylococcal nuclease, where the *cis* form would be stabilized by the sole presence of a β carbon on the residue that precedes the proline.²² Whereas both the wild type and the two mutants K116E and K116M showed a significant predominance of the *cis* form with a relative population superior to 70%, two other mutants K116D and K116N provided exceptions to this simple rule with a *cis* population limited to 30%. In our peptide, despite the β -carbon on both residues preceding Pro3 and Pro6 and the important structural constraints imposed by the disulfide bridge, relative populations determined for the *cis* form of both prolines indicate that the *cis* form is not as strongly favored as would be predicted by the β -carbon rule (Table 3). The ready chemical synthesis of the peptide will allow an extensive verification of this β -rule.

NMR Results for the Reduced Peptide. Originally, the splitting in the HPLC pattern was attributed to the *cis/trans* isomerization of a proline residue slowed down by steric constraints induced by cyclization.⁸ Our NMR analysis demonstrated that the conformation of Pro3 induces a global change in the peptide, giving a structural basis for the HPLC behavior. However, the role of the disulfide bridge is not entirely clear. HPLC analysis of the reduced peptide shows one single peak at all temperatures, but two opposite interpretations are possible: either the proline isomerization is fast on the HPLC time scale, and this both for Pro3 and Pro6, or the minority forms are not significantly populated anymore, and one observes one single peak containing only the all-*trans* form.

In order to discern between both possibilities, the reduced peptide was studied by NMR.²⁴ Analysis of the NMR spectra revealed the presence of four proline residues, of which two could readily be assigned to Pro3_{tt} and Pro6_{tt} (strong α – δ

(23) (a) Kallen, J.; Walkinshaw, M. D. *FEBS Lett.* **1992**, *300*, 286. (b) Ke, H.; Mayrose, D.; Cao, W. *Proc. Natl. Acad. Sci. U.S.A.* **1993**, *90*, 3324. (c) Kakalis, L. T.; Armitage, I. M. *Biochemistry* **1994**, *33*, 1495.

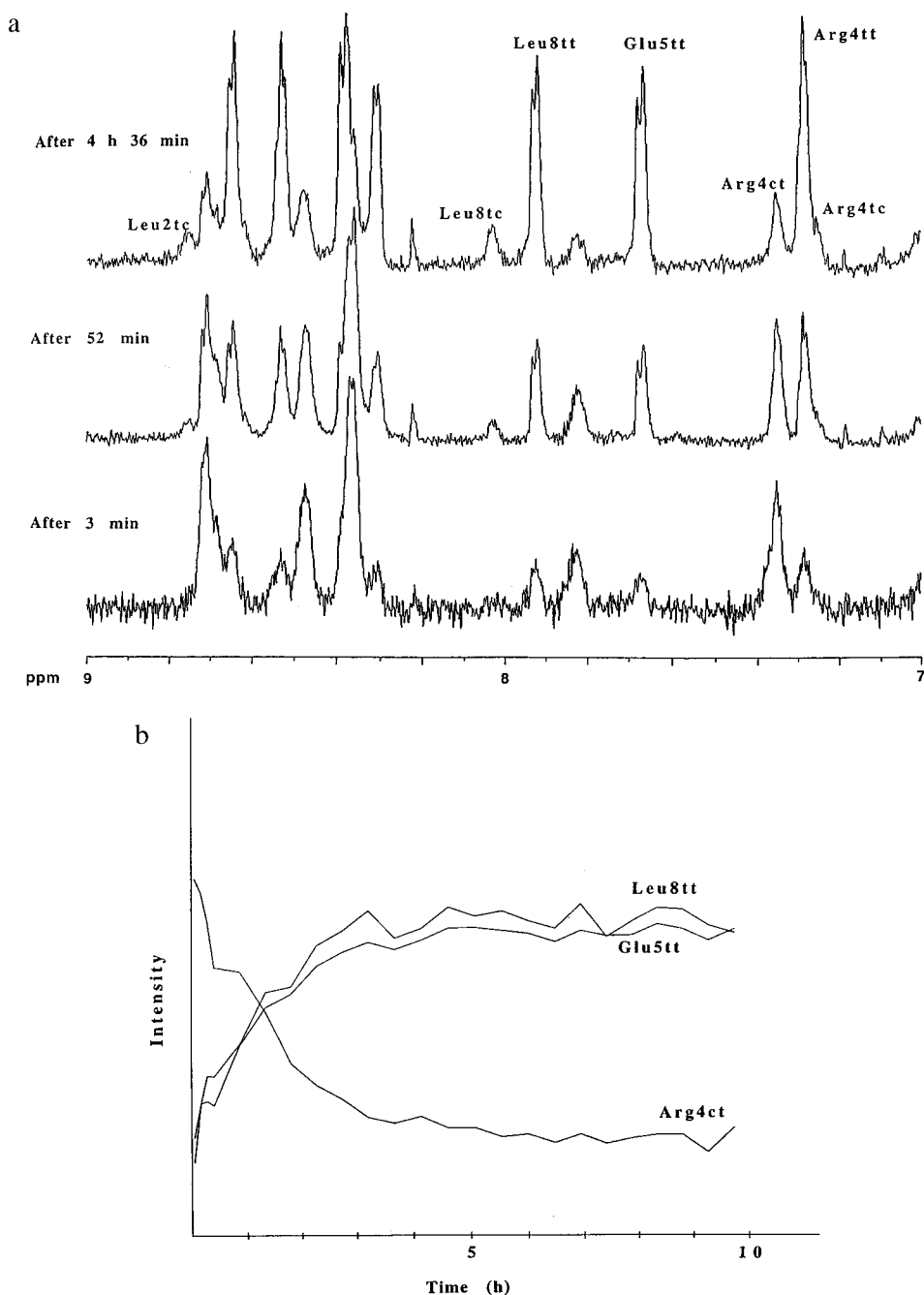


Figure 6. (a) NMR spectra, obtained from the second eluted HPLC peak corresponding to the *cis-trans* form, showing the interconversion between the three forms *cis-trans*, *trans-trans*, and *trans-cis* and collected at different time periods—3 min, 52 min, 4 h 36 min—with 128 scans for the first one and 1024 scans for the others. We observe here the NH resonances. (b) Buildup of the intensities of Leu8tt, Glu5tt, and Arg4ct NH peaks as a function of time.

Table 3. Relative Proportions of the Different Conformers in a Water/Acetonitrile or an Aqueous Solution Evaluated from Results Obtained by HPLC and NMR^a

		H ₂ O	CD ₃ CN
HPLC	tt + tc:ct	69:31	71:29
NMR	tt:tc:ct	60:12:28	69:9:22
	tt + tc:ct	72:28	78:22

^a Ratios were calculated by manual integration of HPLC peaks at 0 °C of 20 μ L of NMR samples in H₂O and in H₂O/CD₃CN, or by integration of glycine geminal cross-peaks from the 400-ms NOESY spectra.

contacts). No clear NOE connectivities could be observed for the two remaining Pro spin systems, but on the basis of chemical shift identity with the protons of Pro3ct and Pro6tc in peptide **I**, we tentatively assigned them to Pro3 in the ct form and Pro6

in the tc form. The fact that only four and not six proline residues could be distinguished indicates a conformational independence of both proline residues in the three forms of the reduced peptide, in contrast with the pronounced dependence in the cyclic peptide. Attribution of the other spin systems confirmed that reduction of the disulfide bridge leads to a peptide where the structure of the N- and C-extremities is only dependent on the conformation of Pro3 and Pro6, respectively. The Leu2 line of the forms tt and tc could not any longer be distinguished in the reduced peptide. A similar conclusion was reached for the spin systems of Leu8 and Gly7, where always two TOCSY lines were observed corresponding to the (tt + ct) molecules or the tc molecule. However, estimation of the relative populations of the conformers by HPLC or NMR was not feasible anymore.

Relieving the constraint of the Lys116–Pro117 containing loop in Staphylococcal nuclease²⁵ yielded a protein where the Lys–Pro bond was only observed in the *trans* form. The situation with the peptide under study here is different: although the structural constraint imposed by the disulfide bridge plays an important role at the level of the activation barrier, the different minority forms (ct and tc) remain present at concentrations observable by NMR.

Conclusion

Whereas HPLC analysis of the cyclized peptide (Cys-Leu-Pro-Arg-Glu-Pro-Gly-Leu-Cys) indicates the presence of two separate conformers with a ratio of 69:31, analysis of ¹H NMR spectra reveals the existence of at least three different isomers in H₂O in a ratio of 60:28:12. Based on the typical NOE connectivities for *cis*- and *trans*-Xaa–Pro peptide bonds, the major isomer was found to be the all-*trans* conformer, whereas in the two minor isomers the peptide bonds Leu–Pro or Glu–Pro are in the *cis* conformation. The isomer with both prolyl peptide bonds in the *cis* conformation could not be detected in these conditions.

The kinetic study showed that the more intense HPLC peak contains the *trans–trans* and *trans–cis* forms whereas the minor HPLC peak contains the *cis–trans* form. We conclude that the proline in position 3 plays the dominant role in the structure of the peptide. This conclusion was confirmed by the structural study which showed that this proline in position 3 determines the conformation of both N- and C-terminal residues.

The study of the reduced peptide indicates that the disulfide bridge is a second important structural element. Removing the

(24) The NMR study of the reduced peptide has been performed at pH 2 and 3.5, pH for which cyclization or dimerization of the peptide is unlikely, and in two solvents, H₂O and H₂O/CD₃CN, no differences were observed under these conditions.

(25) Hodel, A.; Kautz, R. A.; Adelman, D. M.; Fox, R. O. *Protein Sci.* **1994**, *3*, 549.

structural constraint imposed by the cyclization lowers the activation barrier of the interconversion of the proline in position 3. The Pro3 isomerization becomes too fast to be observed on the HPLC time scale. The NMR study showed the presence of both *cis* and *trans* form for the proline in position 6 and the structural independence of the N- and C-terminal parts of the peptide.

We believe that a detailed description of the peptide under its different conformations can lead to a deeper understanding of the complex structural role of the proline residue. The ready chemical synthesis of the peptide brings an extensive verification of the β rule into the realm of possibilities. Moreover, as the proline residues are necessarily solvent-exposed, this peptide forms an ideal substrate to examine the catalytic activity of proline *cis/trans* isomerase. The interaction between PPIases and the peptide in its oxidized and reduced forms is currently under investigation in our laboratory in order to investigate how the activation energy barrier is lowered under the effect of the enzymes.

Acknowledgment. We thank E. Diesis for his help during the course of the synthesis and HPLC analysis work. The 600-MHz facility used in this study was funded by the Région Nord–Pas de Calais (France), the CNRS, and the Institut Pasteur de Lille.

Supporting Information Available: Table giving the ¹H chemical shifts measured (ppm) for the peptide at pH 2.5 in a mixed H₂O/CD₃CN solution, with tt, ct, and tc respectively indicating the *trans–trans*, *cis–trans*, and *trans–cis* forms of the peptide and a list of distance constraints introduced in X-PLOR software for structures generation of the *trans–trans* molecule, with (2.0 0.0 0.8) indicating that distances must be found between 2 and 2.8 Å (3 pages). See any current masthead page for ordering and Internet access instructions.

JA960257Q